World Journal of Advanced Research and Reviews
eISSN: 2581-9615 CODEN (USA): WJARAI
Cross Ref DOI: 10.30574/wjarr
Journal homepage: https://wjarr.com/

(RESEARCH ARTICLE)

Check for updates

Cell viability studies using human gingival fibroblast, human oral fibroblast cells and mechanical characterization of Calcite/Zincite nanoparticles

Sampath Kumar L *, Shantha V and Janardhana K

Department of Mechanical Engineering, Sir M. Visvesvaraya Institute of Technology, Bangalore, Karnataka, India.

World Journal of Advanced Research and Reviews, 2022, 16(03), 812–824

Publication history: Received on 12 October 2022; revised on 26 December 2022; accepted on 29 December 2022

Article DOI: https://doi.org/10.30574/wjarr.2022.16.3.1443

Abstract

Antibiotics are rapidly being replaced with nanoparticles (NPs) in order to eradicate bacteria and other organisms. Nanotechnology, in particular, could be useful in the fight against bacterial pandemics. Although the precise processes are still unknown, it is now understood that metal ion release, the induction of oxidative stress, and non-oxidative mechanisms all contribute to NPs' antibacterial effects. Because many gene alterations in the same bacterial cell are needed for the numerous concurrent modes of action against microorganisms, it is challenging for bacteria to develop NP resistance. As a result, this study also focuses on analyzing the antibacterial activity of the created nanoparticles. The use of PMMA in dentistry demonstrates the necessity for fillers to be added to PMMA to improve its performance. Nano fillers such as ZnO and $CaCO_3$ have unique uses in the field of dentistry due to their advanced features, which include antibacterial activity. However, no study has been conducted to yet on the synthesis of the nanomaterial composed of calcium carbonate and zinc oxide. As a result, an attempt is made in this study, which combines calcium carbonate (calcite) and zinc oxide (zincate), synthesized using precipitation method. Various amounts of human gingival fibroblasts (HGF) and human oral fibroblasts (HOF) were applied to test samples and found as non-toxic. The density increase for composites made by using precipitation method, NPs is about 45% of the PMMA. Shore hardness tests reveal an increasing trend in the hardness of the composites up to 4.5%.

Keywords: MTT Assay; Human gingival fibroblasts; Human oral fibroblasts; Density; Hardness

1 Introduction

Antibiotics are rapidly being replaced with nanoparticles (NPs) in order to eradicate bacteria and other organisms. Nanotechnology, in particular, could be useful in the fight against bacterial pandemics. Examples of the use of NPs to prevent bacterial infections and improve health include antibacterial vaccines, antibiotic distribution systems, bacterial detection systems, microbial diagnostics, and antibacterial coatings for implantable devices and pharmaceutical materials. Although the precise processes are still unknown, it is now understood that metal ion release [1], the induction of oxidative stress [2], and non-oxidative mechanisms [3] all contribute to NPs' antibacterial effects. Because many gene alterations in the same bacterial cell are needed for the numerous concurrent modes of action against microorganisms [4], it is challenging for bacteria to develop NP resistance. As a result, this study also focuses on analyzing the antibacterial activity of the created nanoparticles.

Counting live cells after staining with a vital dye has traditionally been used to determine the in vitro harmful effects of unknown substances. Alternative techniques include counting using automated counters and others that depend on dyes and cellular activity, as well as measuring the incorporation of radioisotopes as a measure of DNA synthesis. Utilizing mitochondrial dehydrogenases, the MTT method can assess the activity of live cells. The MTT technique produces repeatable results and is easy to use. MTT, also known as 3-[4, 5-dimethylthiazol-2-yl]-2, 5-diphenyl tetrazolium bromide, is the main ingredient. It is a water-soluble tetrazolium salt that produces a yellowish solution

* Corresponding author: Sampath Kumar .L

when made in salt solutions or media without phenol red. The mitochondrial dehydrogenase enzymes of live cells cleave the tetrazolium ring of dissolved MTT to produce an insoluble purple formazan (Figure 1). It is possible to dissolve this water-insoluble formazan using DMSO, acidified isopropanol, or other solvents (Pure propanol or ethanol). A spectrophotometric analysis of the resultant purple solution is performed. The amount of formazan generated changes in direct proportion to the number of cells, providing information on the extent of the test material's effects [5].

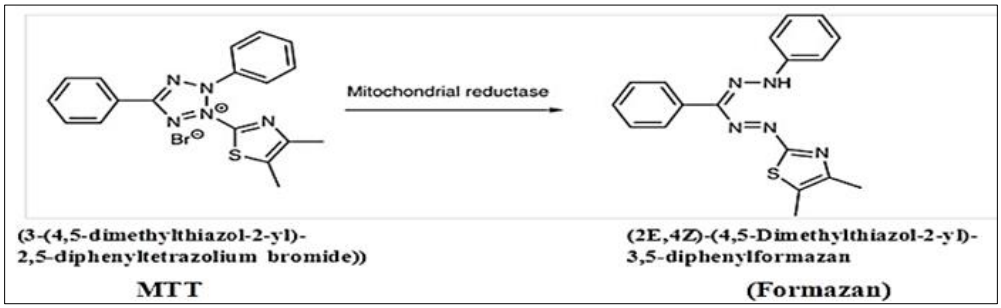

Figure 1 Structure of MTT and Formazan

PMMA is employed in the majority of prosthetic dental applications such as artificial teeth, dentures, bases, retainers, crowns (temporary or provisional), repair, and even research [6-10]. Although the properties are suitable for application, the wear and tear [11, 12], reduction in mechanical properties, and so on are causing researchers to work on the development of newer biomaterials using PMMA reinforced with some of the nano materials that can enhance the thermal and mechanical properties of the PMMA base [13-15]. The goal here is to locate the best nano materials to add into the PMMA base so that the characteristics are improved and the newer biomaterial may be utilized extensively in dental applications. The composite made using PMMA reinforced with various calcite-zincate NP compositions. Mechanical characterization of manufactured composites is performed to determine the application-oriented aspects of the composites in terms of the mechanical properties sought by prosthetic dental applications. The MTT Assay and mechanical.

2 Material and methods

Nanoparticles used for the evaluation of MTT assay and mechanical characterization I the continued work of NPs prepared by green synthesis [16] are considered. The synthesized NPs were analysed for cell viability for Human gingival fibroblasts and Human oral fibroblasts cell lines which were procured from the sources listed in the table 1. The NPs were mixed with PMMA in 0.75:1 ratio and samples were prepared to evaluate the mechanical characterization.

2.1 Materials and method used to analyze cell viability

The materials used for the cell viability studies are tabulated in table 1.

Table 1 List of materials used for the cell viability studies

Sl. No	Particulars	Source	Catalogue No
1	T25 flask	Falcon	353108
2	FGM	Gibco	1932403
3	RPMI media	Gibco	1898961
4	Trypsin EDTA 0.05%	Gibco	1897336
5	FBS	Gibco	10438034
6	Penstrep	Gibco	1924793
7	Sterile 96 well plate	Thermo Scientific	167425
8	MTT reagent	Sigma	MICBX8173V
9	DMSO	Sigma-Aldrich	D2650

10	Potassium chloride	Fisher scientific	19255
11	Sodium chloride	SDFCL	40123K05
12	Disodium phosphate	Fisher scientific	27735
13	Monopotassium phosphate	Fisher scientific	19465
14	1000µl tips	Genaxy	GENUT 1000C
15	200µl tips	Genaxy	GENUT 200C
16	Microcentrifuge tubes	X pet	MCT-1.7-B
17	Serological pipettes	Eppendorf	F000085L
18	Filtration unit	Thermo Scientific	5660020
19	Human Gingival fibroblast	ATCC	PCS-201-018
20	Human Oral fibroblast	Sciencell Research Lab	

2.1.1 Sample preparation:

DMSO was used to create 32 mg/mL stocks for cytotoxicity tests. Using fibroblast growth media as the treatment, serial two fold dilutions from 320 g/mL to 10 g/mL were created [17] is as shown in figure 2.

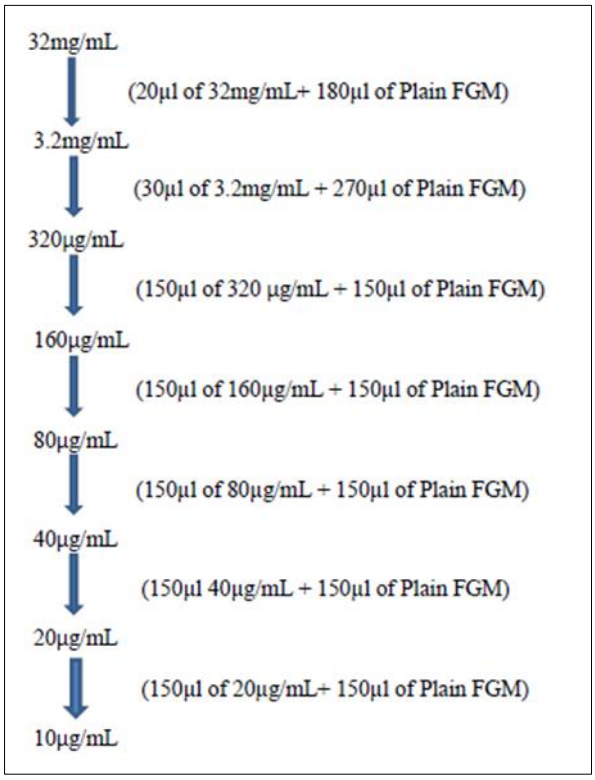

Figure 2 Sample preparation flowchart

2.1.2 Cell lines and culture medium

In fibroblast growth medium (FGM) supplemented with growth factors, penicillin (100 IU/ml), and streptomycin (100 g/ml) in a humidified environment of 5% CO_2 at 37 °C, human gingival fibroblast and human oral fibroblast cell lines were grown until confluent. Cell dissociating solution (0.2% trypsin, 0.02% EDTA, and 0.05% glucose in PBS) was used to separate the cell. The cells are centrifuged and tested for viability. Additionally, 30,000 cells/well on a 96-well plate were planted and cultured for 24 hours in a 37 °C, 5% CO_2 incubator [18].

2.1.3 Procedure

Using appropriate medium containing 10% FBS, the monolayer cell culture was trypsinized and the cell count was increased to 3 x 10^5 cells/ml. A 100 l portion of the diluted cell suspension (30,000 cells/well) was put to each well of the 96-well microtiter plate. When a partial monolayer had developed after 24 hours, the supernatant was removed. The monolayer was then washed once with medium and 100 µl of various test drug concentrations were placed on top of the partial monolayer on microtiter plates. The plates were then incubated for 24 hours at 37°C in a 5% CO_2 environment. Following incubation, the test solutions in the wells were removed, and each well received 100 l of MTT (5 mg/10 ml of MTT in PBS). At 37°C and 5% CO_2, the plates were incubated for 4 hours. In order to dissolve the formazan that had developed the supernatant was taken out, 100 µl of DMSO was added, and the plates were gently agitated. A microplate reader at a wavelength of 590 nm was used to measure the absorbance. The formula (Eq. no – 1) was used to compute the percentage growth proliferation, and the data for the dose-response curves for each cell line were used to calculate the concentration of the test agent required to promote or inhibit cell growth by 50% [19 – 22].

Calculating Inhibition: % Inhibition = [(OD of sample-OD of Control) / OD of Control x 100] - - - - (1)

2.2 Mechanical Characterization

The following steps were used to prepare the composites.

- It was chosen to use a cold cure self-polymerizing acrylic material which is appropriate for all sorts of repairs to acrylic dentures, for the NPs processes were combined in the 5ml ethanol.
- After that, the mixture was sonicated for 5 minutes with a sonication device.
- The PMMA is then mixed with the 0.75:1.00 polymers to liquid ratio.
- NPs were added in percentages of 0.2%, 0.4%, 0.6%, 0.8%, 1.0%, and 1.2% after monomer was added to assure polymerization, and the mixture was then poured onto an open rectangular die and allowed to polymerize.
- The heat from the die is released, and the composite is prepared and removed.
- The PMMA composite augmented with calcite/zincate nanoparticles immersed in water, was then allowed to cool for 120 minutes.
- The appropriate specimens for mechanical evaluation were produced utilizing the laser cutting method once the composite was thoroughly prepared [23].

2.2.1 Density and Porosity measurements

The created composite's features are reflected in the physical quality of density. The word weight fraction is used to indicate the matrix and reinforcement percentage in line with volume fraction or fabrication while performing the property calculations. The displacement technique is regarded as the fundamental approach when values derived from density measurements of composites are tabulated. By comparing the theoretical density of the composite with the observed density using the rule of mixing, the porosity in the composites can then be estimated.

- A = PMMA+0.2% (calcite-zincate) NPs
- B = PMMA+0.4% (calcite-zincate) NPs
- C = PMMA+0.6% (calcite-zincate) NPs
- D = PMMA+0.8% (calcite-zincate) NPs
- E = PMMA+1.0% (calcite-zincate) NPs
- F = PMMA+1.2% (calcite-zincate) NPs

Digital density testers that employ the Archimedes principle were used to measure densities. After recording the difference between the two figures, the actual mass value was divided by it. In the beginning, weights were calculated using two different mediums, namely water and air.

The following procedure is followed to measure the density

- The machine uses deionized water and air weighted air as its two media and is based on the Archimedes principle.
- The specimen's weight in each media was taken into account and noted for various combinations.
- The applicable density kit was used to measure density. The accuracy values of the digital scales are approximately 0.0001 g.

2.2.2 Hardness measurement

The shore durometer is used to test the hardness of semi-rigid and hard plastic materials; it should be calibrated to the ISO 868:2003 standard. When a force is applied, a steel rod that is shaped like a needle pin (30o cone) enters the material and the depth of penetration is recorded on a scale of 0 to 100. A consistent force of 44.64N is applied during the allotted time of 15s. At room temperature, measurements were taken. Each reinforcement mixture underwent fifteen trials. The process is as outlined in figure 3.

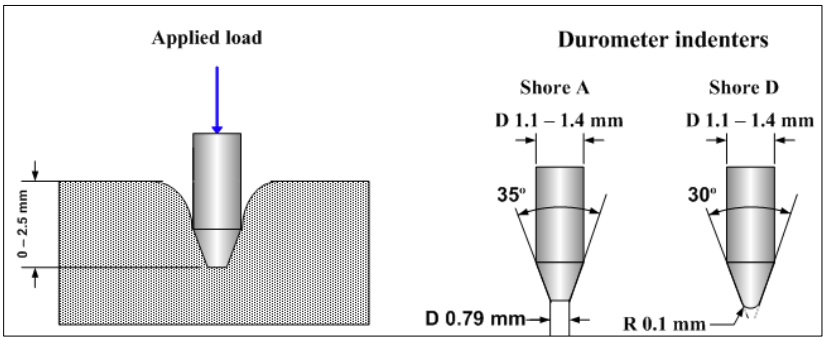

Figure 3 Durometer hardness test

3 Results and discussion

3.1 MTT assay

Figure 4 shows the impact of calcite-zincate NPs on the HGF cells' ability to proliferate. The effect on cell proliferation is shown to be extremely little at concentrations between 10 and 20 g/ml. However, when the concentration of NPs rises, cell growth is inhibited. At a concentration of 320 g/ml, it is shown that cell viability is decreased by about 48%. Additionally, the cell morphology was examined for all NP concentrations, and it was shown that the cell morphology for 10 and 20 g/ml did not alter (figure 6 b-c, 7 b - c). However, at concentrations more than that or when cells are exposed to more than 40 g/ml, a morphological change in the cells is observed (figure 6 d – 6 g). Additionally, fewer cells may be visible. The percentage inhibition may be used to evaluate the toxicity of the NPs; as the inhibition did not exceed 50%, the NPs can be regarded as non-toxic. The cytoplasm of the cells under consideration is unaffected by the reduced NP content. The release of LDH (Lactate Dehydrogenase), which increases at greater concentrations, may be the source of the reduced inhibition. The production of Reactive Oxygen Species (ROS) at larger concentrations is then seen, demonstrating that NPs behave toxically at increasing concentrations.

By treating HOF cells with various NP concentrations, the MTT test is carried out using a same technique. The findings of the MTT experiment are shown in the table 3 and the images in figure 7 a– 7g with regard to percentage inhibition, cytotoxicity, and cell viability.

Table 2 Human Gingival Fibroblasts (HGF)

Compound name	Conc.in µg/ml	OD at 590nm	% Inhibition	OD at 590nm	% Inhibition	OD at 590nm	% Inhibition	Mean % Inhibition	% Cell Viability	Standard Deviation
Control	0	0.715	0.00	0.726	0.00	0.738	0.00	0.00	100.00	0.00
NPs	10	0.689	3.64	0.710	2.20	0.717	2.85	2.90	97.10	0.72
	20	0.635	11.19	0.627	13.64	0.646	12.47	12.43	87.57	1.22
	40	0.610	14.69	0.624	14.05	0.610	17.34	15.36	84.64	1.75
	80	0.564	21.12	0.564	22.31	0.561	23.98	22.47	77.53	1.44
	160	0.481	32.73	0.476	34.44	0.452	38.75	35.31	64.69	3.11
	320	0.439	38.60	0.427	41.18	0.445	39.70	39.83	60.17	1.30

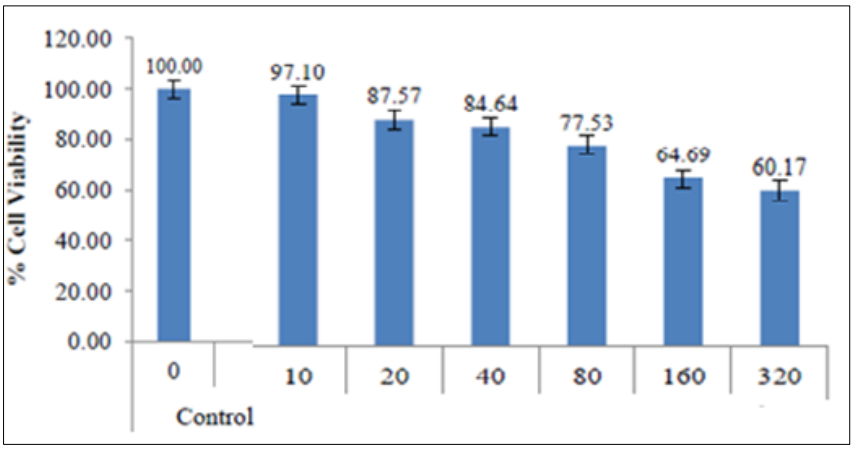

Figure 4 MTT Assay using Human Gingival Fibroblasts cells

Table 3 List of materials used for the cell viability studies

Human Oral Fibroblasts (HOF)										
Compound name	**Conc.in µg/ml**	**OD at 590nm**	**% Inhibition**	**OD at 590nm**	**% Inhibition**	**OD at 590nm**	**% Inhibition**	**Mean % Inhibition**	**% Cell Viability**	**Standard Deviation**
Control	0	0.512	0.00	0.537	0.00	0.529	0.00	0.00	100.00	0.00
NPs	10	0.689	3.64	0.710	2.20	0.717	2.85	2.90	97.10	0.72
	20	0.635	11.19	0.627	13.64	0.646	12.47	12.43	87.57	1.22
	40	0.610	14.69	0.624	14.05	0.610	17.34	15.36	84.64	1.75
	80	0.564	21.12	0.564	22.31	0.561	23.98	22.47	77.53	1.44
	160	0.481	32.73	0.476	34.44	0.452	38.75	35.31	64.69	3.11
	320	0.439	38.60	0.427	41.18	0.445	39.70	39.83	60.17	1.30

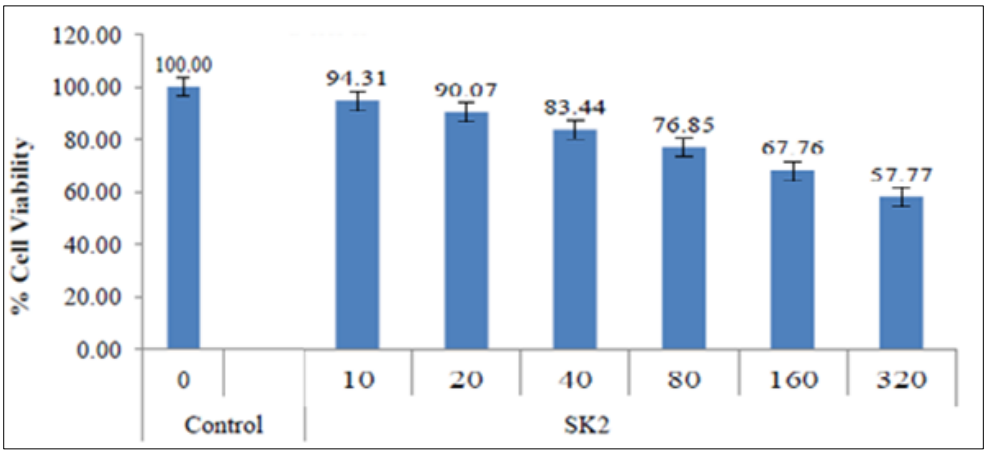

Figure 5 MTT Assay using Human oral Fibroblasts cells

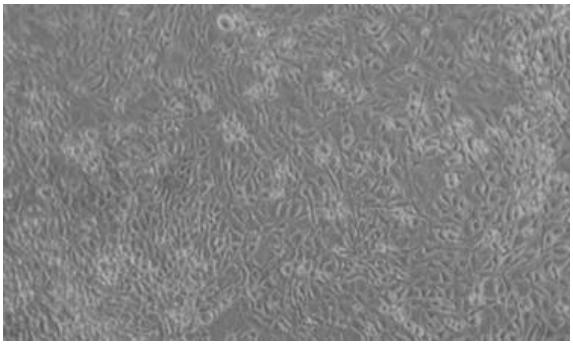

Figure 6 a control

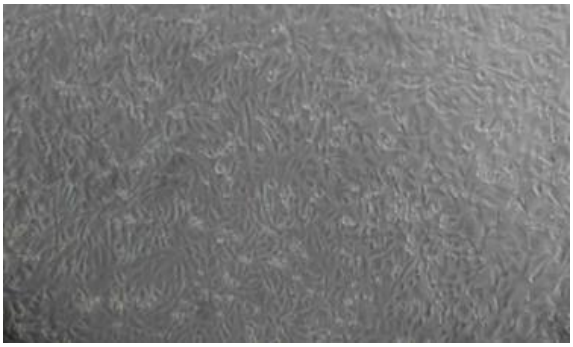

Figure 6 b 10 µg/ml

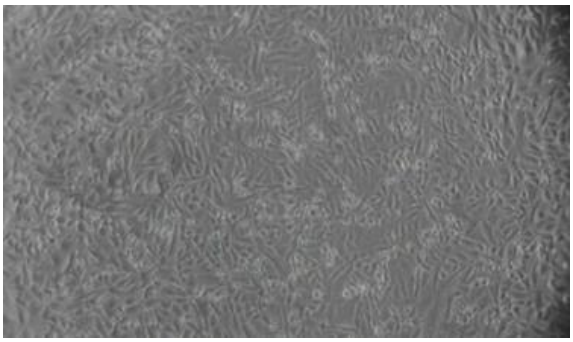

Figure 6 c 20 µg/ml

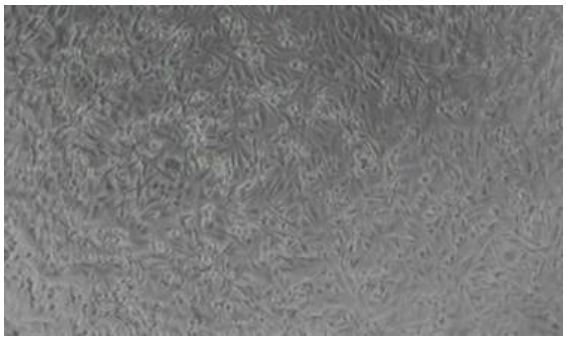

Figure 6 d 40 µg/ml

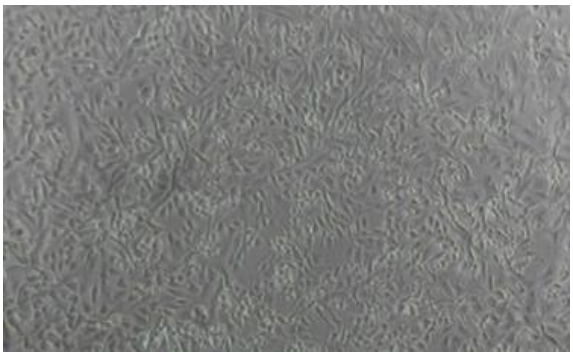

Figure 6 e 80 µg/ml

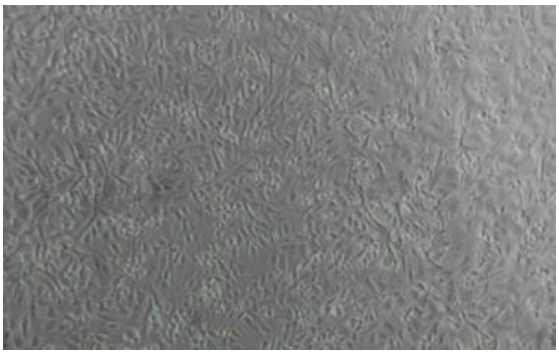

Figure 6 f 160 µg/ml

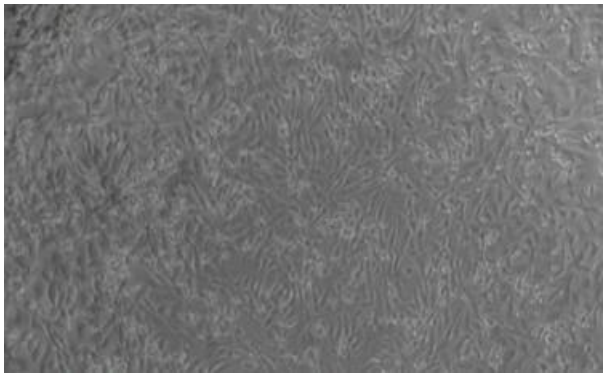

Figure 6 f 320 µg/ml

Figure 6 Changes in HGF cell morphology and number of cells a. control b. 10 µg/ml c. 20 µg/ml d. 40 µg/ml e. 80 µg/ml f. 160 µg/ml g. 320 µg/ml (treated with green synthesized NPs)

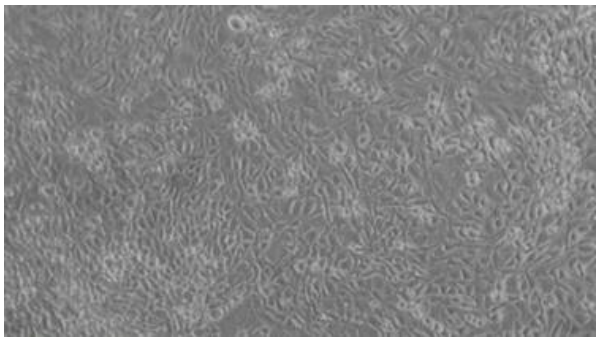

Figure 7 a control

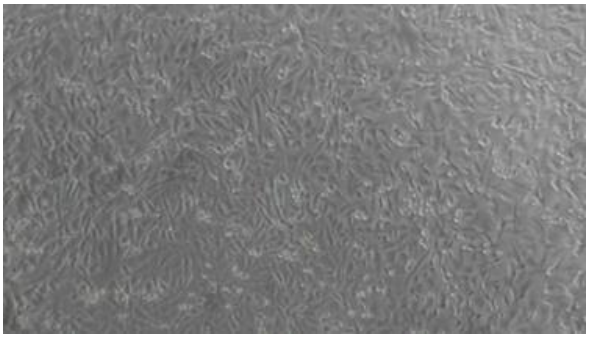

Figure 7 b 10 µg/ml

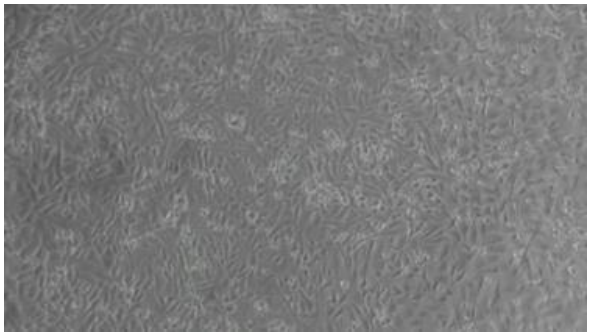

Figure 7 c 20 µg/ml

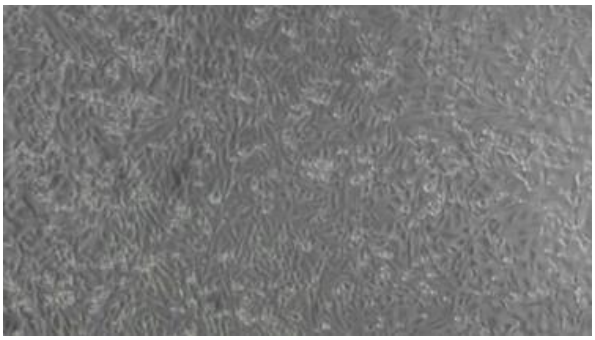

Figure 7 d 40 µg/ml

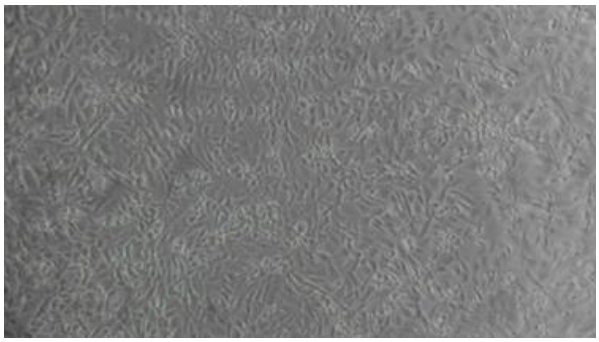

Figure 7 e 80 µg/ml

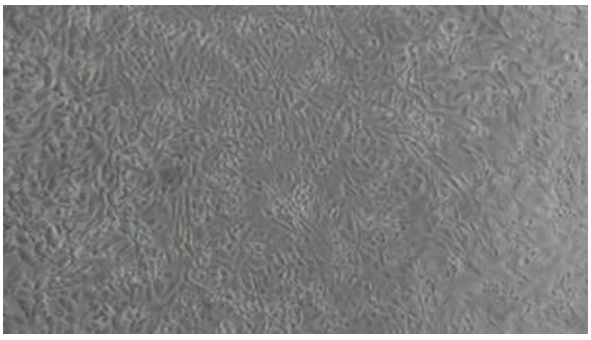

Figure 7 f 160 µg/ml

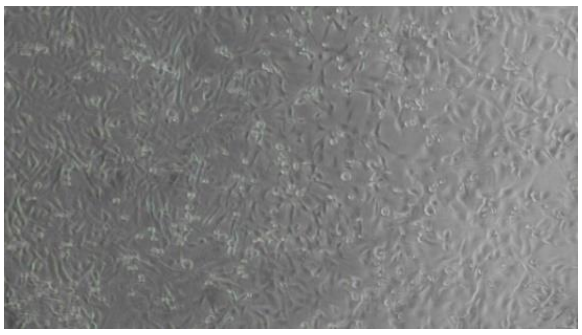

Figure 7 f 320 µg/ml

Figure 7 Changes in HOF cell morphology and number of cells a. control b. 10 µg/ml c. 20 µg/ml d. 40 µg/ml e. 80 µg/ml f. 160 µg/ml g. 320 µg/ml (treated with green synthesized NPs)

3.2 Mechanical Characterization

It is evident that the PMMA here, as well as in composites made with various concentrations of green generated NPs, lacks a crystalline structure and is therefore classified as amorphous. The illustration shows and verifies the existence of green synthetic calcite-zincate nanoparticles in the matrix of polymer. All of the available peaks show that the NPs

have a spherical structure. Many peaks, related to diffraction may be observed, with the first and second peak matching to the lattice planes of calcite-zincate (111 and 200). Both crystalline and amorphous patterns may be seen in the composite patterns along with this two-phase structure. Broad peaks indicated the polymer's amorphous character, and the hexagonal wurtzite structure's usual pattern indicated the presence of calcite-zincate NPs [24, 25]. The pattern refers to the structure of polymer, which is ordered and disordered in the amorphous state, and exhibits the appearance of three wide peaks. The amorphous halo is produced by the distance between the individual polymer chains.

3.2.1 Density and Porosity measurements

Although there isn't much of a difference in the densities of different composition composites (table 3), the rise in density shows (figure 8) that during polymerization, NPs were inserted into the open gaps in the long chain of the polymer. There is no remaining monomer at the conclusion of polymerization, as shown by the XRD graph as well (figure 9). Additionally, since the holes have been filled with NPs, there are no longer any trapped areas where food, germs, or any type of fungus may grow. The material becomes friendlier to oral mucosa due to vibration dampening, which increases E modulus, followed by a sharp decrease in cross-linking level. In light of these findings, PMMA/calcite-zincate NPs can be used instead of PMMA because of their increased density and lower risk of allergic responses.

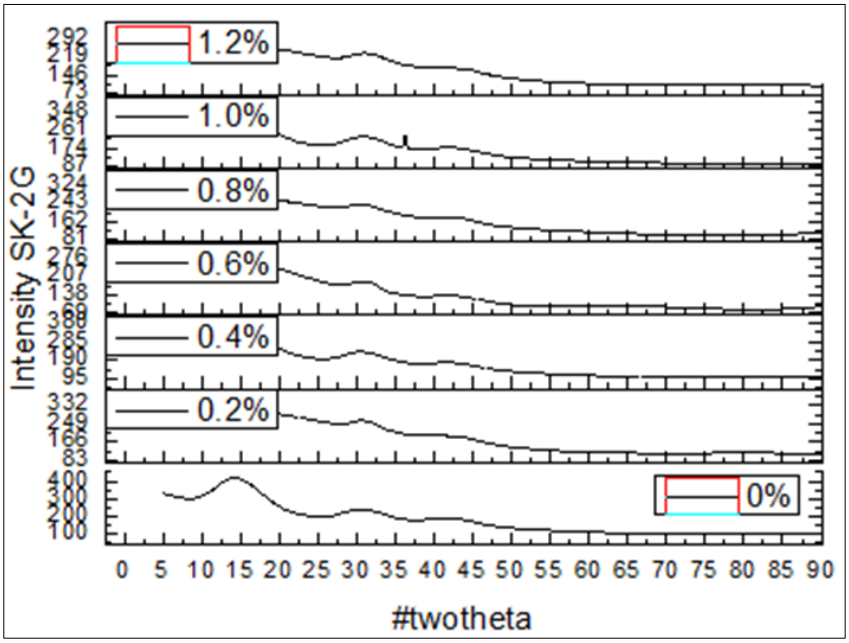

Figure 8 XRD graphs for 0%. 0.2%, 0.4%, 0.6%, 0.8%, 1.0% and 1.2% PMMA-calcite/zincate NPs

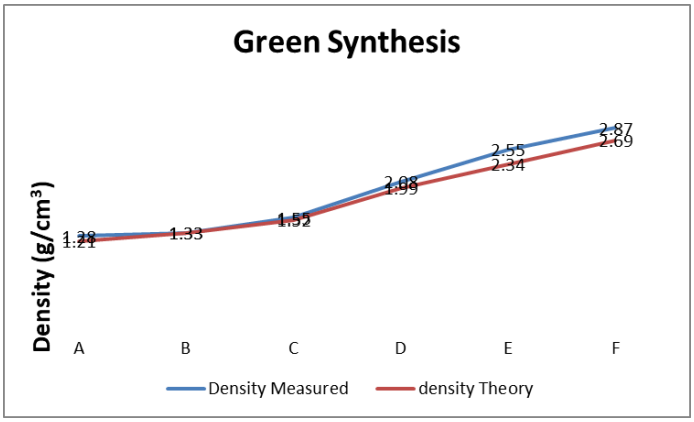

Figure 9 Density values for different compositions of NPs

Table 4 Density of different compositions of composites with nano calcite-zincate NPS (chemical synthesized)

Composition	Density for each trial (grams/cc)	Density (0.93) Measured	Density (grams/cc) Theoretical
A	1.35	1.28	1.21
	1.21		
	1.26		
B	1.32	1.33	1.33
	1.3		
	1.31		
C	1.39	1.55	1.52
	1.69		
	1.56		
D	1.91	2.08	1.99
	2.17		
	2.16		
E	2.64	2.55	2.34
	2.41		
	2.60		
F	2.83	2.87	2.69
	2.87		
	2.91		

3.2.2 Hardness Measurements

The examination of the hardness of PMMA reinforced with calcite-zincate nanoparticles is tabulated in table 4 and depicted in figure 10. When compared to the beach hardness values of composites with various compositions, it is observed that the base matrix (PMMA) has a shore hardness value of 82 shore units.

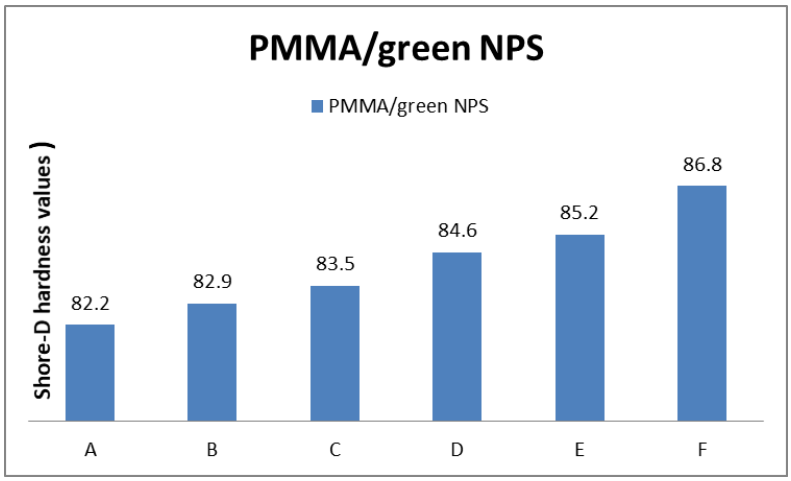

Figure 10 Hardness values of PMMA/NPs

Table 5 Shore-D hardness values of composites

Composition	PMMA/green NPS
A	82.2
B	82.9
C	83.5
D	84.6
E	85.2
F	86.8

The difference in hardness values up to 0.6% of reinforcements (both) are negligible, whereas the overall difference from 0 to 1.2% reinforcements is evident when looking at the shore-D hardness values. The total increase in the hardness values accounts for 4.5% in chemically produced NPs, which is rather noticeable. The hardness values for green synthesized NPs increased overall by 5.6%, which is greater than the composites made with NPs that were made chemically.

Increased hardness makes it easier for the prosthesis to resist surface scuffs and microcracks, which suggests that the growth of fungus biofilm will be particularly hampered on the prepared composite's surface. Additionally, the rise in polymer composite hardness values is taken into account as a technique of assessment to measure the polymer conversion process in acrylic material. As a result, it can be concluded that the hardness values rely on the amount of monomer that is still present after polymerization [26].

4 Conclusion

Various amounts of human gingival fibroblasts (HGF) and human oral fibroblasts (HOF) were applied to test samples SK2 and SK2G for a 24-hour period. As the inhibition did not reach 50%, there was no detectable cytotoxicity. Since the samples' cell viability was more than 50%, they can be regarded as non-toxic.

For the prepared green NPs composite, the density measurements indicate an increase, but only up to 0.8% reinforcements. As compared to PMMA, the density of composites containing green generated NPs rose by 56%. Even at the reinforcing level of up to 1.2%, shore hardness tests reveal an increasing trend in the hardness of the composites. The hardness of composite with green NPs was increased by up to 5.6%.

Compliance with ethical standards

Disclosure of conflict of interest

No conflict of interest statement.

References

[1] Nagy A, Harrison A, Sabbani S, Munson RS Jr, Dutta PK, Waldman WJ. Silver nanoparticles embedded in zeolite membranes: release of silver ions and mechanism of antibacterial action. Int J Nanomedicine. 2011;6: 1833–1852.

[2] Gurunathan S, Han JW, Dayem AA, Eppakayala V, Kim JH. Oxidative stress-mediated antibacterial activity of graphene oxide and reduced graphene oxide in Pseudomonas aeruginosa. Int J Nanomedicine. 2012; 7:5901–5914.

[3] Leung YH, Ng AM, Xu X, et al. Mechanisms of antibacterial activity of MgO: non-ROS mediated toxicity of MgO nanoparticles towards Escherichia coli. Small. 2014, 10(6):1171–1183.

[4] Jung WK, Koo HC, Kim KW, Shin S, Kim SH, Park YH. Antibacterial activity and mechanism of action of the silver ion in Staphylococcus aureus and Escherichia coli. Appl Environ Microbiol. 2008;74(7): 2171–2178.

[5] Crouch, S.P.M. et al. (1993). The use of ATP bioluminescence as a measure of cell proliferation and cytotoxcity. J. Immunol. Meth.160, 81–8.

[6] Al-Harbi, F. A., Abdel-Halim, M. S., Gad, M. M., Fouda, S. M., Baba, N. Z., AlRumaih, H. S., & Akhtar, S. (2018). Effect of Nanodiamond Addition on Flexural Strength, Impact Strength, and Surface Roughness of PMMA Denture Base. Journal of Prosthodontics. doi:10.1111/jopr.12969.

[7] Cierech, M., Wojnarowicz, J., Szmigiel, D., Bączkowski, B. O. H. D. A. N., Grudniak, A. M., Wolska, K. I., Łojkowski, W., & Mierzwińska-Nastalska, E. L. Ż. B. I. E. T. A. (2016). Preparation and characterization of ZnO/PMMA resin nanocomposites for denture bases. Acta of Bioengineering and Biomechanics, 18(2), 31–41. https://doi.org/10.5277/ABB-00232-2014-04.

[8] Gad, M., Rahoma, A., Al-Thobity, A. M., & ArRejaie, A. (2016). Influence of incorporation of ZrO2 nanoparticles on the repair strength of polymethyl methacrylate denture bases. International Journal of Nanomedicine, Volume 11, 5633–5643. doi:10.2147/ijn.s120054

[9] Zidan, S., Silikas, N., Haider, J., Alhotan, A., Jahantigh, J., & Yates, J. (2020). Evaluation of Equivalent Flexural Strength for Complete Removable Dentures Made of Zirconia-Impregnated PMMA Nanocomposites. Materials, 13(11), 2580. doi:10.3390/ma13112580.

[10] Sihama Issa Salih, Jawad Kadhum Oleiwi, Qahtan Adnan Hamad. Investigation of Fatigue and Compression Strength for the PMMA Reinforced by Different System for Denture Applications. International Journal of Biomedical Materials Research. Vol. 3, No. 1, 2015, pp. 5-13. doi: 10.11648/j.ijbmr.20150301.13.

[11] Chaijareenont, P., Takahashi, H., Nishiyama, N., & Arksornnukit, M. (2012). Effect of different amounts of 3-methacryloxypropyltrimethoxysilane on the flexural properties and wear resistance of alumina reinforced PMMA. Dental Materials Journal, 31(4), 623–628. doi:10.4012/dmj.2012-056.

[12] Alamgir, M., Mallick, A., Nayak, G. C., & Tiwari, S. K. (2019). Development of PMMA/TiO2 nanocomposites as excellent dental materials. Journal of Mechanical Science and Technology, 33(10), 4755–4760. doi:10.1007/s12206-019-0916-7.

[13] Ergun, G.; Sahin, Z.; Ataol, A.S. The effects of adding various ratios of zirconium oxide nanoparticles to poly(methylmethacrylate) on physical and mechanical properties. Journal of Oral Science, Vol. 60, No. 2, 304-315, 2018, doi.org/10.2334/josnusd.17-0206.

[14] Al-Karam, L.Q., & M.Majeed, S. (2019). Evaluation the mechanical properties of PMMA / ZrO2 nanoparticles for dental application. International Journal of Research in Pharmaceutical Sciences. DOI:10.26452/IJRPS.V10I3.1409, Corpus ID: 201297459

[15] Hammani, S., Barhoum, A., & Bechelany, M. (2017). Fabrication of PMMA/ZnO nanocomposite: effect of high nanoparticles loading on the optical and thermal properties. Journal of Materials Science, 53(3), 1911–1921. doi:10.1007/s10853-017-1654.

[16] Sampath,Shantha,Hariharan (2022) Characterization and Antimicrobial Activity Studies of calcite and zincite nanoparticles by green synthesis,International Journal of Innovative Research in Advanced Engineering Volume 9, Issue 10 of 2022 pages 426 – 434 https://doi.org/10.26562/ijirae.2022.v0910.03.

[17] Gonzalez, R.J. and Tarloff, J.B. (2001) Evaluation of hepatic sub cellular Fractions for alamar blue and MTT reductase activity. Toxicology in vitro.15, 259-9.

[18] Lundin, A. et al. (1986) Estimation of biomass in growing cell lines by adenosine triphosphate assay, Methods enzymol.133,27-42.

[19] Kangas, L. et al. (1984) Bioluminescence of cellular ATP: A new method for Evaluating cytotoxic agents in vitro. Med. Biol. 62, 338–43

[20] F F Denizot, R R Lang. Rapid colorimetric assay for cell growth and survival. Modifications to the tetrazolium dye procedure giving improved sensitivity and reliability. Journal of Immunological Methods 1986-05-22.

[21] Hattori, N. et al. (2003) Enhanced microbial biomass assay using mutant luciferase resistant to benzalkonium chloride. Anal. Biochem.319287–95.

[22] Cell Viability and Proliferation. Mark Frei, BioFiles v6 n5, 17–21.

[23] McCabe JF, Walls AW (2013) Applied dental materials. Wiley, London.

[24] Ni, M., & Ratner, B. D. (2008). Differentiating calcium carbonate polymorphs by surface analysis techniques-an XPS and TOF-SIMS study. Surface and Interface Analysis, 40(10), 1356–1361. doi:10.1002/sia.2904.

[25] Hammani, S., Barhoum, A., & Bechelany, M. (2017). Fabrication of PMMA/ZnO nanocomposite: effect of high nanoparticles loading on the optical and thermal properties. Journal of Materials Science, 53(3), 1911–1921. doi:10.1007/s10853-017-1654.

[26] Alobiedy, A. N., Alhille, A. H. and Al-Hamaoy, A. R. (2019) "Mechanical Properties Enhancement of Conventional Glass Ionomer Cement by Adding Zirconium Oxide Micro and Nanoparticles", Journal of Engineering, 25(2), pp. 72–81. doi: 10.31026/j.eng.2019.02.05.